

## Relation between the Multi-Regge Model and the Amati-Bertocchi-Fubini-Stanghellini-Tonin Pion-Exchange Multiperipheral Model\*

GEOFFREY F. CHEW, TERENCE ROGERS,† AND DALE R. SNIDER

*Department of Physics and Lawrence Radiation Laboratory,  
University of California, Berkeley, California 94720*

(Received 8 April 1970)

The 1962 Amati-Bertocchi-Fubini-Stanghellini-Tonin (ABFST) multiperipheral model, with a kernel based on an up-to-date guess for the elastic  $\pi\pi$  cross section, is used to illuminate certain controversial concepts that have arisen in multi-Regge models. The small magnitude of the elastic  $\pi\pi$  cross section above the region of prominent resonances is related to the small diffraction-dissociation cross section and to the small Pomeron coupling constant in the Chew-Pignotti (CP) model. Although lower trajectories in the multi-Regge kernel give an inadequate representation of low-subenergy resonances, we show that an artificial CP-model input can be found which roughly simulates the resonance component of the ABFST kernel. Byproducts of our investigations are (1) a generalization of the Berestetsky-Pomeranchuk formula that provides a practical basis for exact numerical evaluation of the ABFST model at any energy, and (2) a perturbative analysis of diffractive dissociation (d.d.) which reconciles a small d.d. cross section at accessible energies with a total cross section that becomes entirely of the d.d. type in the extreme high-energy limit.

### I. INTRODUCTION

AN attempt has been made during the past two years to elucidate the dynamical status of the Pomeron and other high-ranking Regge trajectories through the study of multiparticle production processes via multi-Regge-pole models.<sup>1-7</sup> Interesting results have been achieved, but the shaky underpinning of multi-Regge dynamics has left room for skepticism about their significance. We here revive the 1962 Amati-Bertocchi-Fubini-Stanghellini-Tonin (ABFST) multiperipheral model<sup>8</sup> based on (non-Regge) pion exchange in an effort to illuminate certain controversial aspects of the 1968 Chew-Pignotti (CP) multi-Regge-pole model.<sup>1,4-6</sup> The qualitative conclusions from the latter survive, and there emerges a more specific and, perhaps, more believable picture of the underlying mechanism.

It is an established experimental fact that if the final particles from a multiple-production reaction are ordered according to longitudinal momenta, the mean subenergy of a neighboring pion pair is less than or of the order of 1 GeV.<sup>9</sup> This experimental importance of small subenergies in the multiperipheral chain has three immediate consequences that undermine confidence in

the CP model while at the same time supporting the ABFST model:

1. Kinematic approximations depending on large values of subenergies are unjustified.
2. A multi-Regge-pole model based on leading trajectories requires an extreme and perhaps unreasonable significance for duality: an adequate Regge description of the lowest-energy resonances.
3. A lower-lying trajectory containing a low-mass particle may be more important than high-lying trajectories containing no low-mass particle; that is, a representation in the original "peripheral" sense based on nearby poles in momentum transfer may be more relevant than a representation based on high-ranking poles in angular momentum.

We are thus led to reconsider the model based on pion-pole dominance that was introduced in 1962 by ABFST.<sup>8</sup> The small pion mass motivates the assumption that the dominant multiperipheral chain is the one shown in Fig. 1, which maximizes the number of pion-exchange links in a collision of the type

$$A+B \rightarrow A+B+2(N+1) \text{ pions.} \quad (1.1)$$

Every second link is to be approximated by a pion pole, allowing the following factorization of the amplitude:

$$\mathcal{F}_{AB \rightarrow AB+n\pi} \approx f_{\pi A}(s_A, \theta_A) \frac{1}{t_1 - m_\pi^2} f_{\pi\pi}(s_1, \theta_1) \frac{1}{t_2 - m_\pi^2} \cdots \frac{1}{t_{N+1} - m_\pi^2} f_{\pi B}(s_B, \theta_B), \quad (1.2)$$

where  $f_{\pi\pi}(s, \theta)$  is the elastic  $\pi\pi$  amplitude at c.m. angle  $\theta$  and energy  $s^{1/2}$ , and  $f_{\pi A, B}$  is the corresponding amplitude for pions colliding with particles of type  $A, B$ . Since the  $s_i$  are not large on the average, we shall not use a Regge representation for these two-particle  $\rightarrow$

\* Work supported in part by the U. S. Atomic Energy Commission.

† Present address: Cavendish Laboratory, Cambridge, England.

<sup>1</sup> G. F. Chew and A. Pignotti, Phys. Rev. **176**, 2112 (1968).

<sup>2</sup> G. F. Chew, F. E. Low, and M. L. Goldberger, Phys. Rev. Letters **22**, 208 (1969).

<sup>3</sup> I. G. Halliday and L. M. Saunders, Nuovo Cimento **60**, 494 (1969).

<sup>4</sup> L. Caneschi and A. Pignotti, Phys. Rev. **180**, 1525 (1969); **184**, 1915 (1969).

<sup>5</sup> G. F. Chew and W. R. Frazer, Phys. Rev. **181**, 1914 (1969).

<sup>6</sup> W. R. Frazer and C. H. Mehta, Phys. Rev. Letters **23**, 258 (1969).

<sup>7</sup> J. Ball and G. Marchesini, Phys. Rev. **188**, 2209 (1969); **188**, 2508 (1969).

<sup>8</sup> L. Bertocchi, S. Fubini, and M. Tonin, Nuovo Cimento **25**, 626 (1962); D. Amati, A. Stanghellini, and S. Fubini, *ibid.* **26**, 6 (1962).

<sup>9</sup> Z. Ajduk, L. Michejda, and W. Wójcik, INR (Warsaw) Report No. 1088/VI/PH (unpublished).

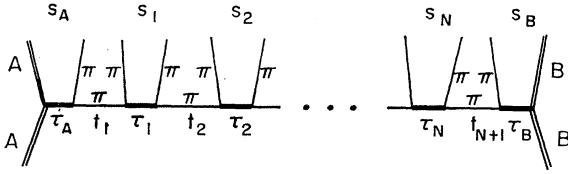


FIG. 1. Diagram representing the ABFST-model amplitude for the process  $A+B \rightarrow A+B+2(N+1)\pi$ .

two-particle amplitudes, but instead will employ a realistic guess based on a combination of experimental and theoretical sources. We shall not assume that the low-energy resonance components of these two-particle amplitudes are adequately described on the average by a Regge representation, as was conjectured by Chew and Pignotti.<sup>1</sup>

The model amplitude (1.2) is constructed so as to have the pion poles at the correct positions with the correct residues, but the implied prescription for moving away from the poles is arbitrary. We shall identify  $\theta_i$  as the angle, in the c.m. system of the outgoing  $i$ th pion pair, between the direction of the outgoing pions and the direction of the spatial components of the adjacent momentum transfers. This prescription leads to a simple relation between the kernel of the multiperipheral integral equation and the elastic  $\pi\pi$  cross section. Other equally plausible prescriptions lead to less manageable relations.

In the ABFST model<sup>8</sup> the pion plays the role of a zero-spin elementary particle, a fact which implies a counterpart Bethe-Salpeter equation. "Reggeizing" the pion links would break the Bethe-Salpeter correspondence and still leave a tractable problem,<sup>10-12</sup> but the logic behind such an "improvement" is not presently clear. If a motivation emerges, pion Reggeization can and will be studied in the future.

Both in the ABFST pion-exchange model and in the multi-Regge-pole model, the result of summing all partial cross sections leads to a total cross section with Regge asymptotic behavior. Any model based on the iteration of a multiperipheral kernel yields output Regge poles, but the (input) multi-Regge-pole model explicitly characterizes the kernel through Regge trajectories and residues and thereby closes an immediate bootstrap cycle. The bootstrap implications of the ABFST model are not fundamentally different but are indirect—requiring an additional link that proceeds outside the model and involves crossing. It would be convenient if duality were to permit the multi-Regge shortcut, but, as shown in Appendix C, the resulting errors are quantitatively inadmissible.

A further simplification important to the CP model was the neglect of phase-space correlation between

adjacent momentum transfers in the multiperipheral chain. It was thereby possible to factor the kernel, to average over separate momentum transfers, and thus to define effective coupling constants. These constants are related so indirectly to Regge residues, even assuming duality, that so far they have been determined only by fitting multiple-production data. However, since kernel factorization is equivalent to the trace approximation for the Fredholm determinant, and in the ABFST model the trace approximation turns out to be tolerable, we have the possibility of calculating the effective CP coupling constants from the ABFST kernel, that is, from the  $\pi\pi$  elastic cross section. In particular, we shall be able to understand a vital feature of the CP model, the small value of the internal Pomeron coupling, in terms of the small high-energy tail of the elastic  $\pi\pi$  cross section.

A well-known and powerful technique for studying the ABFST model is to write an integral equation for the imaginary part of the forward amplitude and to diagonalize the equation by a suitable transformation. The transformation is from the energy  $s$  to the Toller variable  $\lambda$ : a "higher angular momentum" in the  $t$  channel. This approach directly yields the asymptotic  $s$  properties of the cross section, but is less well adapted to studying finite-energy properties of the model, particularly if the kernel has a small but nonzero component at high subenergy. Such a component generates fine structure in the output Regge-pole spectrum, so that the physics of finite energies involves the positions and residues of several output poles. We shall consider the diagonalization approach in the final sections of this paper, but in the earlier sections we shall study the ABFST model by more elementary methods.

## II. INDIVIDUAL CROSS SECTIONS FOR MULTIPLE PION PRODUCTION

As the most elementary and straightforward approach to the ABFST model, we present in this section the model prediction for individual production cross sections. The notation will be useful for all subsequent considerations. Referring to Fig. 1, let us define a set of "vertex boost"<sup>10-13</sup> parameters  $q_A, q_1, q_2, \dots, q_N, q_B$  by

$$\cosh q_i = \frac{s_i - t_i - t_{i+1}}{2(-t_i)^{1/2}(-t_{i+1})^{1/2}}, \quad (2.1a)$$

$$\sinh q_A = \frac{s_A - m_A^2 - t_1}{2m_A(-t_1)^{1/2}}, \quad (2.1b)$$

$$\sinh q_B = \frac{s_B - m_B^2 - t_{N+1}}{2m_B(-t_{N+1})^{1/2}}, \quad (2.1c)$$

<sup>10</sup> G. F. Chew and C. DeTar, Phys. Rev. **180**, 1577 (1969).

<sup>11</sup> A. H. Mueller and I. J. Muzinich, Ann. Phys. (N. Y.) (to be published).

<sup>12</sup> M. Ciafaloni, C. DeTar, and M. Misheloff, Phys. Rev. **188**, 2522 (1969).

<sup>13</sup> N. F. Bali, G. F. Chew, and A. Pignotti, Phys. Rev. **163**, 1572 (1967); Phys. Rev. Letters **19**, 614 (1967).

together with the "over-all boost" parameter  $\eta$ :

$$\cosh \eta = \frac{s - m_A^2 - m_B^2}{2m_A m_B}. \quad (2.2)$$

Let us also define quantities  $C_A(s)$ ,  $C(s)$ , and  $C_B(s)$  such that<sup>14</sup>

$$C(s) = (1/16\pi^3)\lambda(s, m_\pi^2, m_\pi^2)\sigma_{e1}^{\pi\pi}(s), \quad (2.3a)$$

$$C_A(s) = (1/16\pi^3)\lambda(s, m_A^2, m_\pi^2)\sigma_{e1}^{\pi A}(s), \quad (2.3b)$$

$$C_B(s) = (1/16\pi^3)\lambda(s, m_B^2, m_\pi^2)\sigma_{e1}^{\pi B}(s), \quad (2.3c)$$

with

$$\lambda(x, y, z) = [x^2 + y^2 + z^2 - 2(xy + xz + yz)]^{1/2}. \quad (2.4)$$

In terms of these quantities, we show in Appendix A

$$\begin{aligned} \sigma_N^{AB}(s) = & \frac{16\pi^3}{\lambda^2(s, m_A^2, m_B^2)} \int ds_A ds_1 ds_2 \cdots ds_N ds_B dt_1 dt_2 \cdots dt_{N+1} \frac{(\eta - q_A - q_1 - q_2 - \cdots - q_N - q_B)^N}{N!} \theta(\eta - q_A - q_1 - \cdots - q_B) \\ & \times \frac{C_A(s_A) C(s_1) \cdots C(s_N) C_B(s_B)}{(t_1 - m_\pi^2)^2 (t_2 - m_\pi^2)^2 \cdots (t_{N+1} - m_\pi^2)^2}. \end{aligned} \quad (2.5)$$

Note that the index  $N$  has been defined so that  $N = -1$  has the significance

$$\sigma_{-1}^{A\pi}(s) = \sigma_{e1}^{\pi A}(s). \quad (2.6)$$

The special case of Eq. (2.5) with  $N=0$  was first written down by Berestetsky and Pomeranchuk.<sup>15</sup>

The derivation of Eq. (2.5) is given in Appendix A for the case of neutral pions. When charge is included it is convenient to diagonalize in the crossed-channel isotopic spin, which may take the values  $I=0, 1, 2$  in the ABFST model because two pions are exchanged between particles  $A$  and  $B$  in the sense of Fig. 2. One then replaces Eq. (2.3a) by

$$C^I(s) = \frac{1}{16\pi^3} \lambda(s, m_\pi^2, m_\pi^2) \sum_{I'} \beta_{II'} \sigma_{e1, I', \pi\pi}(s), \quad (2.3a')$$

where  $\beta_{II'}$  is the isotopic-spin crossing matrix,

$$\beta_{II'} = \begin{pmatrix} \frac{1}{3} & 1 & \frac{5}{3} \\ \frac{1}{3} & \frac{1}{2} & -\frac{5}{6} \\ \frac{1}{3} & -\frac{1}{2} & \frac{1}{6} \end{pmatrix}. \quad (2.7)$$

$$\begin{aligned} F_N(p_1, p_{N+1}) &= F_N^+((p_1 - p_{N+1})^2, p_1^2, p_{N+1}^2) \\ &\equiv \int ds_1 \cdots ds_N C(s_1) \cdots C(s_N) \left(\frac{2}{\pi}\right)^{N-1} \int d^4 p_2 \cdots d^4 p_N \frac{\delta^+((p_2 - p_1)^2 - s_1) \cdots \delta^+((p_{N+1} - p_N)^2 - s_N)}{(p_2^2 - m_\pi^2)^2 \cdots (p_N^2 - m_\pi^2)^2}, \end{aligned} \quad (3.1)$$

corresponding to Fig. 3, where all lines refer to pions. Although not explicitly so represented in its arguments,  $F_N^+$  is nonzero only for positive timelike components of  $(p_{N+1} - p_1)$ . The normalization is such that, by comparison with

<sup>14</sup> If the incident particles ( $A, B$ ) are not pions, Eqs. (2.3b) and (2.3c) should be interpreted so that the cross sections  $\sigma_{\pi A}^{e1}(s)$  include  $\delta$ -function contributions at  $s = m_A^2$ , corresponding to an end link in Fig. 1 leading to one particle rather than two.

<sup>15</sup> V. B. Berestetsky and I. Ya. Pomeranchuk, Zh. Eksperim. i Teor. Fiz. **12**, 752 (1961) [Soviet Phys. JETP **39**, 1078 (1960)]; Nucl. Phys. **22**, 629 (1961).

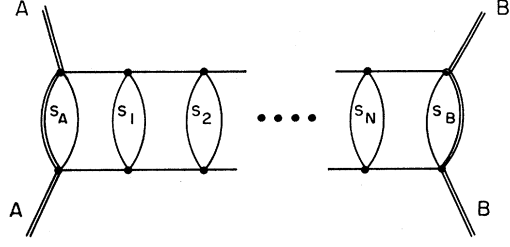


FIG. 2. Diagram representing the cross section obtained by squaring the ABFST amplitude of Fig. 1.

that the amplitude (1.2) leads to the following formula for the cross section  $\sigma_N^{AB}$  to produce  $N$  internal pairs of pions (see Fig. 2):

There will be a corresponding replacement of  $C_A$  and  $C_B$  that depends on the isotopic spin of particles  $A$  and  $B$ .

The formulas of this section give the physical content of the ABFST model in terms of input elastic cross sections. At any finite energy, only a finite number of the output inelastic cross sections  $\sigma_N^{AB}$  are nonzero, so with a sufficiently powerful computer the theoretical task would now be finished, nothing but elementary quadrature remaining. Already at lab energies  $\lesssim 20$  GeV, however, the number of important  $N$  values is sufficiently large that important collective effects appear in the total cross section, effects which are unlikely to be illuminated by a simple-minded term-by-term evaluation. It is thus worthwhile to study the summation over  $N$  by the integral equation technique of ABFST.

### III. RECURSION RELATION AND ABFST INTEGRAL EQUATION

Following ABFST and using the notation of Sec. II, we define a Lorentz-invariant function of two four-vector variables,

Eq. (2.5) (see Appendix A),

$$F_N^+(s, m_\pi^2, m_\pi^2) = [\lambda(s, m_\pi^2, m_\pi^2)/16\pi^3] \sigma_{N-2}^{\pi\pi}(s), \quad (3.2)$$

or, more generally,

$$\sigma_N^{AB}(s) = \frac{16\pi^3}{\lambda(s, m_A^2, m_B^2)} \int ds_A ds_B C_A(s_A) C_B(s_B) \left(\frac{2}{\pi}\right)^2 \int d^4 p_1 d^4 p_{N+1} \times \frac{\delta^+((p_1 - p_A)^2 - s_A) \delta^+((p_B - p_{N+1})^2 - s_B)}{(p_1^2 - m_\pi^2)^2 (p_{N+1}^2 - m_\pi^2)^2} f_N(p_1, p_{N+1}). \quad (3.3)$$

Observe that although the definition (3.1) implies for the special case  $N=1$  that the function

$$F_1^+(s, t, t') = C(s) \quad (3.4)$$

is independent of  $t$  and  $t'$ , in general, the functions  $F_N^+$  depend on all three scalars.

The functions  $f_N(p, p')$  satisfy the recursion relation

$$f_N(p, p') = \int_{4m_\pi^2}^{\infty} ds_N C(s_N) \frac{2}{\pi} \times \int d^4 p_N \frac{\delta^+((p' - p_N)^2 - s_N)}{(p_N^2 - m_\pi^2)^2} f_{N-1}(p, p_N). \quad (3.5)$$

The upper limit of the  $s_N$  integration is only formally infinite, since  $s_N$  must be less than  $(p - p')^2$  by some finite amount. [This constraint is imposed in the  $p_N$  integration, where it is impossible to simultaneously satisfy the  $\delta$  function and have  $(p - p_N)^2$  above the threshold for the function  $f_{N-1}$  if  $s_N > (p - p')^2$ .]

The definition

$$f(p, p') = \sum_{N=1}^{\infty} f_N(p, p') \quad (3.6)$$

then leads to the ABFST integral equation

$$f(p, p') = f_1(p, p') + \frac{2}{\pi} \int d^4 p'' f(p, p'') K(p'', p'), \quad (3.7)$$

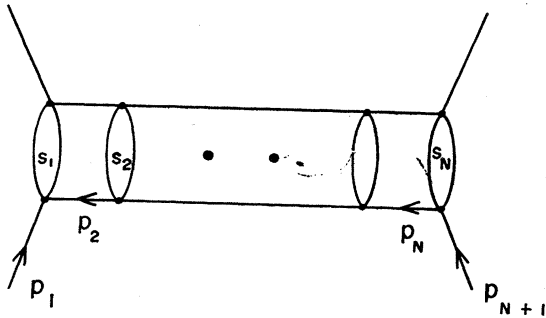


FIG. 3. Momenta and invariants used in the integral equation.

with the kernel

$$K(p'', p') \equiv \int ds' C(s') \frac{\delta^+((p' - p'')^2 - s')}{(p''^2 - m_\pi^2)^2} = \frac{f_1(p'', p')}{(p''^2 - m_\pi^2)^2}. \quad (3.8)$$

Equation (3.2), together with (2.6), implies

$$F^+(s, m_\pi^2, m_\pi^2) = [\lambda(s, m_\pi^2, m_\pi^2)/16\pi^3] \sigma_{\text{tot}}^{\pi\pi}(s), \quad (3.9)$$

whereas replacement of  $f_N$  by  $f$  in Eq. (3.3) yields a total inelastic cross section for a general  $(A, B)$  collision.

If the integral equation (3.7) is solved by iteration and substituted into (3.3), one simply reproduces the sequence of partial cross sections given by (2.5). We propose to study the solution by two other methods. The first method depends on splitting the basic kernel-determining function  $C(s)$  into two parts—one large and one small—and treating the small part as a perturbation. To motivate such a splitting of the kernel, we now examine the structure of  $C(s)$  as revealed by experimental  $\pi\pi$  elastic scattering data.

Figure 4 shows our estimate, based partly on experimental knowledge and partly on the Veneziano model, of the three  $\pi\pi$  elastic cross sections and the three  $C^I$ 's. We have included the following resonances: standard  $\rho$  and  $f$  (both with a 140 MeV width), a broad  $\epsilon$  ( $\Gamma_\epsilon = 450$  MeV) at the  $\rho$  mass, and highly inelastic  $g$  and  $\rho''$ . The assumed properties of these resonances are presented in Table I. We also included a nonresonant  $I=2$  cross section of 8–12 mb and forced the cross sections down to approximately match the Weinberg scattering lengths

TABLE I. Estimated properties of the low-energy  $\pi\pi$  resonances.

Resonance	Mass (GeV)	Full width (GeV)	Elasticity $=\Gamma_{\pi\pi}/\Gamma_{\text{tot}}$	$\sum I\beta_0\sigma_{\text{tot}}^I$ (max) (mb)	$d_{\pi R}^a$
$\rho$	0.765	0.14	1.0	231	0.25
$\epsilon$	0.765	0.45	1.0	26	0.09
$f$	1.26	0.14	1.0	46	0.05
$g$	1.65	0.14	0.35	38	0.04
$\rho''$	1.65	0.14	0.28	7	0.01
					$d^R=0.44$

<sup>a</sup> Evaluated from Eq. (4.20) for  $T=1$  GeV<sup>2</sup>.

at threshold.<sup>16</sup> From Fig. 4 one sees that for  $s > 3 \text{ GeV}^2$ , the resonance fluctuations are expected to be negligible, so that a representation in terms of Regge poles above this energy is valid. One observes, furthermore, that the cross sections for  $s > 3 \text{ GeV}^2$  are expected to be small relative to their values in the region of low-energy resonances. From factorization (and also the intuitive notion that, since the high-energy ratio  $\sigma_{\text{el}}/\sigma_{\text{tot}}$  is  $\frac{1}{6}$  to  $\frac{1}{5}$  for both  $p\bar{p}$  and  $\pi\bar{p}$ , this ratio must have a similar value for  $\pi\pi$ ), we obtain  $\sigma_{\text{tot}}^{\pi\pi} = 16 \text{ mb}$  and  $\sigma_{\text{el}}^{\pi\pi}(\text{asym}) = 2.5\text{--}3.0 \text{ mb}$ . Of course  $\sigma_{\text{el}}^{\pi\pi}(s)$  is not constant, due to the logarithmic shrinkage of the diffraction peak, so we mean these values to hold for  $s \approx 20\text{--}50 \text{ GeV}^2$ .

#### IV. WEAK POMERANCHUK COMPONENT OF ABFST KERNEL AND DIFFRACTIVE DISSOCIATION

The ABFST model, like a multi-Regge model, necessarily implies multiple Pommeranchuk ( $P$ ) exchange. When the model is expressed as an integral equation and then diagonalized, as in Sec. V below, this  $P$  component produces the kernel's rightmost singularity in the  $J$  plane and complicates the leading singularity structure of the output amplitude. The asymptotic behavior of the amplitude at extreme high energies is correspondingly affected.  $P$ -generated singularities have nevertheless been shown in the CP model to be so weak that at moderate energies the  $P$  component of the kernel has relatively minor physical consequence.<sup>1,5</sup> But because the CP model employs dubious approximations to achieve its high degree of tractability, the generality of the "weak Pommeranchuk" notion has not been widely appreciated. In this section we use the ABFST model to study the same question in a different and perhaps more persuasive context.

Rather than working in the  $J$  plane, we shall study in a direct fashion the effect on the moderate-energy total cross section of including or excluding from the ABFST kernel the high-energy tail of the elastic  $\pi\pi$  cross section. Our starting point will be the undiagonalized integral equation (3.7), together with perturbation theory. We show for energies where  $s$  is large but  $\ln s$  is not, that single- $P$  exchange is predicted to be small and multiple- $P$  exchange negligible. Exchange of at least one  $P$  in an inelastic reaction is often characterized as diffractive dissociation (d.d). Hence the objective of this section is to show that moderate-energy d.d. cross sections are relatively small.

The specification of "moderately high" energy is crucial to an understanding of the subtle behavior of d.d. We shall find that the proportion of the total cross section involving at least one  $P$  exchange increases with increasing energy. Eventually this fraction must approach unity, but not until energies at which  $\ln s$  is a large number. In other words, the rate of increase of the d.d. cross section is so small that, even at energies at

<sup>16</sup> S. Weinberg, Phys. Rev. Letters 17, 616 (1966).

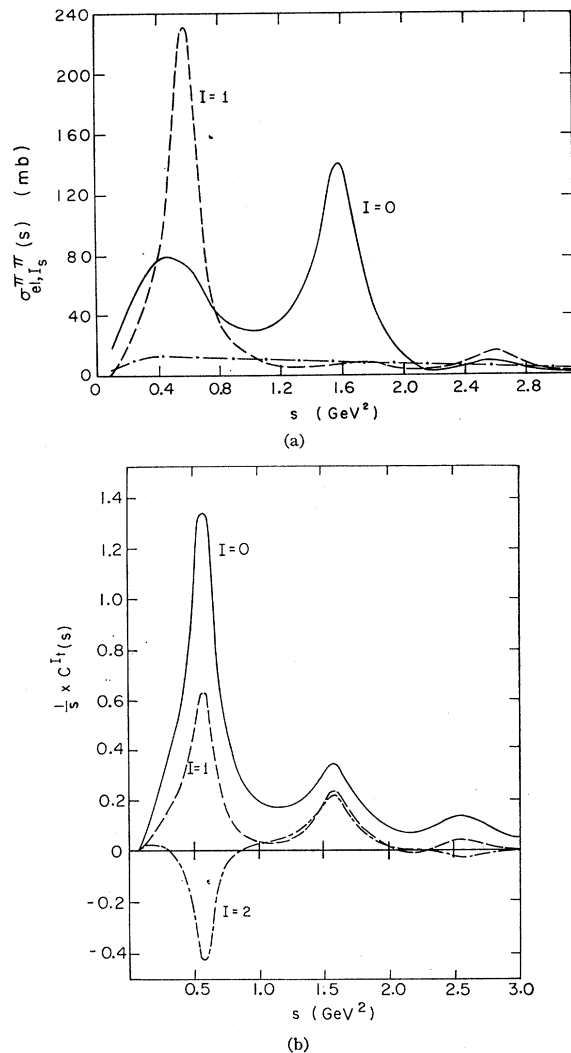


FIG. 4 (a) Assumed  $\pi\pi$  elastic cross sections; (b) functions  $C_I^{\pi\pi}(s)/s$ , given by Eq. (2.3a') with insertion of the cross sections shown in (a).

which Regge behavior of the total cross section is well established (e.g.,  $s \approx 20$ ,  $\ln s \approx 3$ ), the d.d. component remains a minor fraction.

It follows then that any model which attempts to describe the total cross section purely in terms of  $P$  exchange, single or multiple, is inadequate. On the other hand, a crude model may omit  $P$  exchange if one wishes to describe only moderately high energies.

After this lengthy preamble we now proceed to estimate the first-order effect of the Pommeranchuk on the total cross section at energies where  $s$ , but not  $\ln s$ , is large. We shall separate the elastic  $\pi\pi$  cross section into two components—a large low-energy resonance component and a small high-energy tail—and then calculate the effect of omitting or including this tail. We thus begin by writing

$$f_1(s) = f_1^R(s)\theta(s^* - s) + f_1^P(s)\theta(s - s^*), \quad (4.1)$$

where  $s^*$  will usually be taken as about 3 GeV<sup>2</sup> (see Fig. 4). Next we express the integral equation (3.7) symbolically as

$$\begin{aligned} f &= f_1 + fgf_1 \\ &= f_1^R + f_1^P + fg(f_1^R + f_1^P), \end{aligned} \quad (4.2)$$

where  $g$  represents the pion propagator. Let  $f^R$  designate the zeroth-order solution,

$$f^R = f_1^R + f^R g f_1^R. \quad (4.3)$$

Then, to first order in the small quantity  $f_1^P$ ,

$$f \approx f^R + f_1^P + f_1^P g f^R + f^R g f_1^P + f^R g f_1^P g f^R, \quad (4.4)$$

or, also to first order in  $f_1^P$ ,

$$\Delta f = f - f^R \approx f_1^P + f_1^P g f + f g f_1^P + f g f_1^P g f. \quad (4.5)$$

Separating off the first term, which corresponds to elastic scattering, we have for our perturbation estimate of diffractive dissociation

$$\sigma_{\text{d.d.}, \pi\pi} \approx \frac{16\pi^3}{\lambda} \left( \int f_1^P g f + \int f g f_1^P + \int \int f g f_1^P g f \right). \quad (4.6)$$

The first two terms in the parentheses represent dissociation of either one or the other of the two incident

particles, while the third represents dissociation of both. We shall refer to these alternatives as "single dissociation" and "double dissociation," respectively.

We have at the outset agreed to treat the function  $f_1(p, p')$  as depending only on the single scalar  $(p' - p)^2$ . Doing the same for  $f(p, p')$  in Eq. (4.6), we may replace  $f$  through Eq. (3.9) by the total  $\pi\pi$  cross section. Now, suppose we assume that the ABFST model has the capacity to generate the physically observed pion-production cross sections and the corresponding total cross section. Then, to evaluate  $\sigma_{\text{d.d.}, \pi\pi}$  via Eq. (4.6), we do not require the resonance kernel  $f_1^R$ . We can substitute in the observed total cross section. Assuming such capacity for the model, we propose to use the experimental total cross section in Eq. (4.6). The two types of integrals therein are then formally identical to those appearing in Eq. (2.5) for  $N=0, 1$ , except that certain elastic cross sections now become total cross sections.

If at this point we restrict attention to zero isospin in the crossed channel, and correspondingly define

$$C^{\text{tot}}(s) = \frac{\lambda(s, m_\pi^2, m_\pi^2)}{16\pi^3} \sum_{I'} \beta_{0I'} \sigma_{\text{tot}, I'}^{\pi\pi}(s), \quad (4.7)$$

we obtain by appropriate substitutions in Eq. (2.5) the following explicit realization of Eq. (4.6):

$$\begin{aligned} \sigma_{\text{d.d.}, \pi\pi}(s) \approx & 2 \frac{16\pi^3}{\lambda^2(s, m_\pi^2, m_\pi^2)} \int ds_1 C^{\text{tot}}(s_1) \int ds_2 C(s_2) \int \frac{dt}{(t - m_\pi^2)^2} \theta(\eta - q_1 - q_2) + \frac{16\pi^3}{\lambda^2(s, m_\pi^2, m_\pi^2)} \\ & \times \int ds_1 C^{\text{tot}}(s_1) \int ds_2 C(s_2) \int ds_3 C^{\text{tot}}(s_3) \int \frac{dt_1}{(t_1 - m_\pi^2)^2} \int \frac{dt_2}{(t_2 - m_\pi^2)^2} (\eta - q_1 - q_2 - q_3) \theta(\eta - q_1 - q_2 - q_3). \end{aligned} \quad (4.8)$$

Examination of the integrands appearing in (4.8) reveals that the simple pion propagators do not sufficiently cut off the large- $t$  contributions. As written, one finds the important range of  $|t_i|$  to increase indefinitely with increasing  $s$ , in violation of the underlying physical assumption of peripheralism. A related fact discussed below in Sec. V is that the diagonalized ABFST equation is not of Fredholm type unless a  $t$  cutoff is imposed. [The cutoff parameter employed in Sec. V is not precisely equivalent to that used here, because in this section we have neglected the dependence of  $f(p, p')$  on  $p^2$  and  $p'^2$ .] This deficiency presumably arises from our having treated the exchanged pions as elementary. In any event, when evaluating (4.8) we shall employ a simple square cutoff in the  $t$  integrals, recognizing that our original motivating assumption of pion-pole dominance requires that such a cutoff be not much larger than 1 GeV<sup>2</sup>.

To facilitate evaluation of Eq. (4.8), we break the total cross section, and correspondingly  $C^{\text{tot}}(s)$ , into

high- and low-energy components:

$$\sigma_{\text{tot}}^{\pi\pi}(s) = \sigma_{\text{tot}}^R(s) \theta(s^* - s) + \sigma_{\text{tot}}^P(s) \theta(s - s^*). \quad (4.9)$$

The formula for  $\sigma_{\text{d.d.}, \pi\pi}$  then becomes the sum of five terms, which schematically we write as

$$\begin{aligned} \sigma_{\text{d.d.}, \pi\pi} \approx & 2 \int \sigma_{\text{tot}}^R g \sigma_{\text{el}}^P + 2 \int \sigma_{\text{tot}}^P g \sigma_{\text{el}}^P \\ & + \int \sigma_{\text{tot}}^R g \sigma_{\text{el}}^P g \sigma_{\text{tot}}^R + 2 \int \sigma_{\text{tot}}^R g \sigma_{\text{el}}^P g \sigma_{\text{tot}}^P \\ & + \int \sigma_{\text{tot}}^P g \sigma_{\text{el}}^P g \sigma_{\text{tot}}^P. \end{aligned} \quad (4.10)$$

The first term of (4.10) may be described as a "generalized Deck effect,"<sup>17</sup> as depicted in Fig. 5(a). When represented as the reaction  $\pi_A + \pi_B \rightarrow \pi_A^* + \pi_B$ , the mass range here of  $\pi_A^*$  is small [so small when  $R$  is

<sup>17</sup> R. J. Deck, Phys. Rev. Letters **13**, 169 (1964).

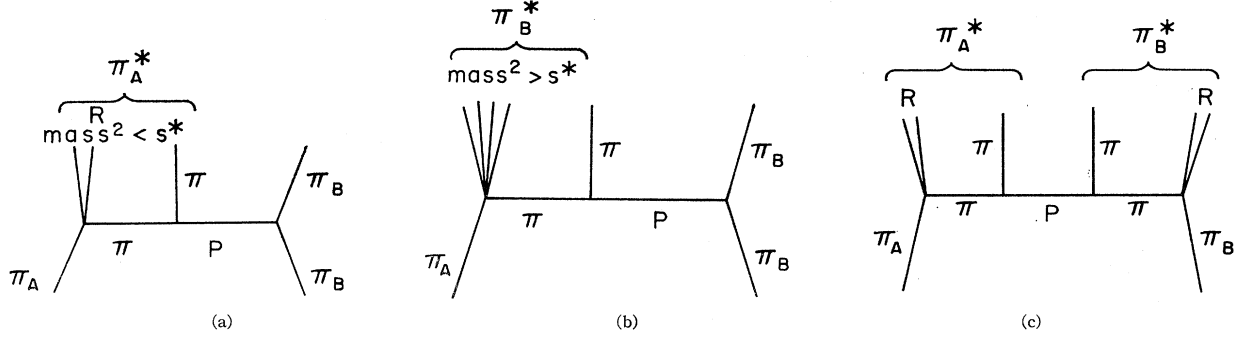


FIG. 5. (a) Singly diffractive generalized Deck effect,  $\pi_A^*$  being a low-mass system; (b) single diffraction dissociation leading to a large-mass  $\pi_B^*$ ; (c) doubly diffractive reaction  $\pi_A + \pi_B \rightarrow \pi_A^* + \pi_B^*$ , where both  $\pi_A^*$  and  $\pi_B^*$  are low-mass systems containing only a few pions.

the  $\rho$  resonance as to allow a  $3\pi(A_1)$  resonance interpretation]. It is well known that the model under study here gives an acceptable description of diffractively produced resonances.<sup>18</sup>

The second term of (4.10) corresponds to Fig. 5(b) and is less easy to identify with a clean physical measurement because the mass of  $\pi_A^*$  is now unbounded. In missing-mass terminology, this second term evidently corresponds to the region of large missing mass, above the prominent individual resonances. Each interval in missing mass yields a contribution to the d.d. cross section that is constant in over-all energy, but since the missing-mass range increases with energy, the total contribution to d.d. from this second term increases with  $s$  and must finally surpass the resonance contribution.

So far only the first term of (4.10) has received systematic experimental study. The final three terms correspond to doubly diffractive dissociation, with or without large masses for  $\pi_A^*$  and  $\pi_B^*$ . Figure 5(c), for example, corresponds to the third term of (4.10), where the masses of both  $\pi_A^*$  and  $\pi_B^*$  are constrained.

In evaluating the integrals we use the following approximations:

$$\sigma_{el}^P(s) \approx \text{const}, \quad (4.11)$$

$$\sigma_{tot}^P(s) \approx \text{const}, \quad (4.12)$$

$$\sigma_{tot}^R(s) \approx \sum_i \sigma_i(\text{max}) \pi \Gamma_i m_i \delta(s - m_i^2), \quad (4.13)$$

where  $m_i$ ,  $\Gamma_i$ , and  $\sigma_i(\text{max})$  are the masses, widths, and peak total cross sections of the important  $\pi\pi$  resonances (see Table I). Since we are concerned only with moderate energies, we neglect the effect of diffraction peak shrinkage on the elastic cross section.

There is no difficulty in numerically evaluating Eq. (4.8), but understanding of the physics is enhanced by further analysis. Let us suppose that  $s \gg s^* \gg T \gg m_\pi^2$ ,  $T$  being the cutoff on the  $t$  integration. Kinematic simpli-

fications explained in Appendix C then lead to the following asymptotic approximations to the five components of Eq. (4.10):

$$2 \int \sigma_{tot}^R g \sigma_{el}^P \approx d^R \sigma_{el}^P, \quad (4.14)$$

$$2 \int \sigma_{tot}^P g \sigma_{el}^P \approx d^P \ln(s/\bar{s}) \sigma_{el}^P, \quad (4.15)$$

$$\int \sigma_{tot}^R g \sigma_{el}^P g \sigma_{tot}^R \approx \frac{1}{2} (d^R)^2 \sigma_{el}^P, \quad (4.16)$$

$$2 \int \sigma_{tot}^R g \sigma_{el}^P g \sigma_{tot}^P \approx \frac{1}{2} d^P d^R \ln(s/\bar{s}) \sigma_{el}^P, \quad (4.17)$$

$$\int \sigma_{tot}^P g \sigma_{el}^P g \sigma_{tot}^P \approx \frac{1}{8} (d^P)^2 \ln^2(s/\bar{s}) \sigma_{el}^P, \quad (4.18)$$

where

$$d^P \equiv (T/16\pi^3) \sigma_{tot}^P, \quad (4.19)$$

$$d^R \equiv \sum_i d_i^R = \sum_i \frac{T}{16\pi^3} \frac{\pi \Gamma_i m_i \sigma_i(\text{max})}{T + m_i^2}. \quad (4.20)$$

The scale parameter  $\bar{s}$  is of the order of magnitude  $(s^*)^2/T$ .

All cross sections, including  $\sigma_{d.d.}$ , refer to the linear combination appearing in (4.7), which at high energies is three times the actual  $\pi\pi$  cross section. To avoid confusion about normalization, it is helpful to think in terms of the ratio of  $\sigma_{d.d.}$  to  $\sigma_{el}$ , which is controlled by the dimensionless quantities  $d^P$  and  $d^R$ . With  $T=1$  GeV<sup>2</sup> and  $\sigma_{tot}^{\pi\pi}=16$  mb, we find from (4.19) the result

$$d^P \approx 0.25, \quad (4.21)$$

while from the  $\pi\pi$  resonance parameters listed in Sec. III, Eq. (4.20) gives (see Table I)

$$d^R \approx 0.44. \quad (4.22)$$

<sup>18</sup> O. Czyzewski, in *Proceedings of the Fourteenth International Conference on High-Energy Physics, Vienna, 1968*, edited by J. Prentki and J. Steinberger (CERN, Geneva, 1968), p. 367.

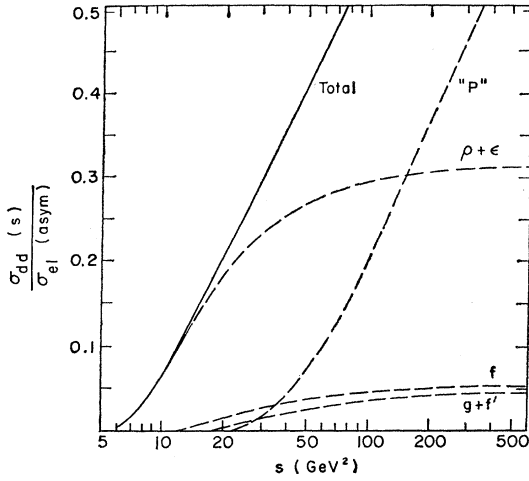


FIG. 6.  $\pi\pi$  diffractive dissociation cross section, normalized to the asymptotic  $\pi\pi$  elastic cross section. Contributions from various parts of  $\sigma_{\text{tot}}^{\pi\pi}$  are shown separately.

With such moderate-sized coefficients one sees from (4.16)–(4.18) that double d.d. is small compared with single d.d. so long as  $\ln s$  is not large.

It is easy now to see that multiple- $P$  exchange is totally negligible. Since in first order single d.d. is larger than double d.d., in second order the largest term is

$$2 \int \sigma_{\text{el}}^P \sigma_{\text{el}}^P \sigma_{\text{tot}}^P,$$

which, by comparison with (4.18), is

$$\frac{1}{4} (d^P)^2 (\sigma_{\text{el}}^P / \sigma_{\text{tot}}^P) \ln^2(s/\bar{s}) \sigma_{\text{el}}^P, \quad (4.23)$$

when the leading power of  $\ln s$  is evaluated. Thus a good estimate of the total moderate-energy d.d. in the ABFST model is given by the first two terms of (4.10), or, more generally, by the first term of (4.8)—which is simply the Berestetsky-Pomeranchuk singly peripheral formula<sup>15</sup> with an elastic cross section at one vertex and a total cross section at the other.

The Berestetsky-Pomeranchuk formula is sufficiently simple that it can be numerically integrated without approximations. In Fig. 6 we show the result of such an integration, still using the simple forms (4.11)–(4.13) but with an exact treatment of phase space and the physical value of  $m_\pi$ .

The result of our estimate is that the moderate-energy d.d. cross section is smaller than the elastic cross section, and thus very small compared with the total. The d.d. production of a fixed interval of missing mass has the same dependence on total energy as the elastic cross section, but the missing-mass spectrum elongates with incident energy, so that the integrated d.d. cross section increases logarithmically. When the integrated d.d. cross section becomes comparable to the total, the perturbation approach of this section becomes invalid,

but from (4.15) and (5.21) we estimate that this will not occur until

$$d^P \ln(s/\bar{s}) \sigma_{\text{el}}^P \approx \sigma_{\text{tot}}^P, \quad (4.24)$$

or, with

$$\begin{aligned} \sigma_{\text{el}}^P / \sigma_{\text{tot}}^P &\approx \frac{1}{6}, \\ \ln(s/\bar{s}) &\approx 24. \end{aligned} \quad (4.25)$$

Thus for all except the highest cosmic-ray energies, it is appropriate to think of the Pomeranchon component of the ABFST kernel as a small perturbation.

## V. DIAGONALIZED EQUATION AND DETERMINATION OF REGGE-POLE POSITIONS

We may use the variables of Bali, Chew, and Pignotti<sup>10,13</sup> to reformulate the ABFST integral equation, which in Eq. (3.7) we have expressed through conventional momentum variables. Diagonalization of the equation is then possible, using the techniques of Refs. 10–12. The result is the same as achieved by the Bethe-Salpeter route,<sup>7</sup> and, now exposing the isospin index, may be written

$$F_I^\lambda(t, t') = F_{I,1}^\lambda(t, t') + \int_{-\infty}^0 dt'' F_I^\lambda(t, t'') K_I^\lambda(t'', t'), \quad (5.1)$$

where the “partial wave”  $F^\lambda$  is defined by

$$F_I^\lambda(t, t') \equiv \int_1^\infty d \cosh \eta \frac{e^{-(\lambda+1)\eta(s, t, t')}}{\lambda+1} F_I^+(s, t, t'), \quad (5.2)$$

with

$$\cosh \eta(s, t, t') = (s - t - t') / 2(tt')^{1/2}, \quad (5.3)$$

a similar projection formula defining the inhomogeneous term  $F_{I,1}^\lambda$ . The projected kernel of the integral equation turns out to be given by

$$\begin{aligned} K_I^\lambda(t'', t') &= \frac{1}{(t'' - m_\pi^2)^2} \\ &\times \int_{4m_\pi^2}^\infty ds C_I(s) \frac{e^{-(\lambda+1)\eta(s, t'', t')}}{\lambda+1}. \end{aligned} \quad (5.4)$$

The appropriate formula to invert the transformation (5.2), given in Ref. 19, is

$$F_I^+(s, t, t') = \frac{1}{2\pi i} \int d\lambda (\lambda+1) \frac{e^{+(\lambda+1)\eta}}{\sinh \eta} F_I^\lambda(t, t'), \quad (5.5)$$

the integration over  $d\lambda$  running over a contour from  $-i\infty$  to  $+i\infty$ , passing to the right of all  $\lambda$  singularities of  $F^\lambda$ . The rightmost  $\lambda$  singularities then control the large- $s$  asymptotic behavior of  $F_I(s, t, t')$ .

Roughly speaking, the  $\lambda$  singularities of  $F_I^\lambda$  arise from two different sources. Branch points already present in

<sup>19</sup> M. Ciafaloni and C. DeTar, Phys. Rev. D 1, 2917 (1970).



the kernel  $K_I^\lambda$  and in the inhomogeneous term  $F_{I,1}^\lambda$  propagate into the solution of the integral equation, whereas poles in  $\lambda$  arise from zeros of the Fredholm determinant—corresponding to solutions of the homogeneous equation. Pole positions thus depend only on the kernel and not at all on the inhomogeneous term. We shall confine our attention here to the question of pole positions, leaving the more difficult question of residues for future investigation.

Equation (5.4) shows that, if the elastic  $\pi\pi$  cross sections are power bounded, the kernel  $K_I^\lambda(t, t')$  is an analytic function of  $\lambda$  for  $\text{Re}\lambda$  sufficiently large. As discussed in Sec. VI, Eq. (6.1), we assume the asymptotic behavior

$$C_I(s) \underset{s \rightarrow \infty}{\sim} C_I \frac{(s/s_0)^{\beta_I}}{\ln(s/s_0)}, \quad (5.6)$$

with

$$\begin{aligned} \beta_0 &= 2\alpha_P(0) - 1 \approx 1, \\ \beta_1 &= \alpha_P(0) + \alpha_\rho(0) - 1 \approx \frac{1}{2}, \\ \beta_2 &= 2\alpha_\rho(0) - 1 \approx 0, \end{aligned} \quad (5.7)$$

$\alpha_P(0)$  and  $\alpha_\rho(0)$  being the zero- $t$  intercepts of the Pomernchuk and  $\rho$  trajectories, respectively. When (5.6) is combined with (5.4), it follows that the right-most  $\lambda$  singularity in  $K_I^\lambda$  is an infinite logarithmic branch point at  $\lambda = \beta_I$ , with strength proportional to  $C_I$ :

$$K_I^\lambda(t, t') \xrightarrow{\lambda \rightarrow \beta_I} \frac{C_I}{\lambda + 1} \left( \frac{(t')^{1/2}}{s_0} \right)^\lambda \frac{(t')^{1/2}}{(t - m_\pi^2)^2} \ln \frac{1}{\lambda - \beta_I}. \quad (5.8)$$

Analytic continuation to the left of this branch point is possible, but we shall be mainly concerned with the region to the right, at least for  $I=0$  and  $I=1$ .

The  $t$  dependence of (5.8) shows that even for  $\text{Re}\lambda > \beta_I$ , the kernel (5.4) is non-Fredholm, the simple inverse power behavior in  $t$  and  $t'$  not being adequate to produce convergence in (5.1). A cutoff of the large- $t$  region is required, just as in Sec. IV, and we shall achieve this by replacing the  $-\infty$  lower limit in (5.1) with  $-\Delta$ , where we expect to choose  $\Delta \lesssim 1 \text{ GeV}^2$ . We shall find, fortunately, that certain important qualitative conclusions can be reached independently of the value of  $\Delta$ .

Once an assumption has been made about  $C_I(s)$ , it is a straightforward matter by numerical computation to determine the Regge poles as values of  $\lambda$  for which the kernel has a unit eigenvalue. Insight into the dynamics is enhanced, however, by considering the trace approximation to the Fredholm determinant, whose vanishing corresponds to the unit eigenvalue:

$$\begin{aligned} D^I(\lambda) &\approx 1 - \text{Tr} K_I^\lambda \\ &= 1 - \frac{1}{\lambda + 1} \int_{-\Delta}^0 \frac{dt}{(t - m_\pi^2)^2} \\ &\quad \times \int_{4m_\pi^2}^\infty ds e^{-(\lambda+1)\eta(s,t)} C_I(s), \end{aligned} \quad (5.9)$$

with  $\cosh \eta(s, t) = 1 - s/2t$ . In this approximation, which we have verified to be reasonably accurate by numerical comparison with the exact solution, the location of Regge poles is reduced to a simple quadrature.

## VI. TRACE APPROXIMATION; COMPARISON WITH CP MODEL

Since resonance fluctuations are expected to be small for  $s > s^* \approx 3 \text{ GeV}^2$ , we break the integral, Eq. (5.9), into low- and high-energy parts, employing a Regge representation for the latter. Here the type of  $J$ -plane singularity appears to be important, so we shall not neglect the effects of diffraction-peak shrinkage. That is, we take

$$C_I(s) \underset{s > s^*}{=} \sum_i \frac{C_i^I}{b_i^I + \ln(s/s_0)} \left( \frac{s}{s_0} \right)^{\beta_i}. \quad (6.1)$$

This form corresponds to an assumed Regge-pole behavior for the elastic  $\pi\pi$  amplitude, with residues varying exponentially with  $\tau$ , leading to a differential cross section

$$\sum_{I'} \beta_{II'} \frac{d\sigma_{I, \text{el}}}{d\tau} \propto \frac{1}{s_0} \sum_{m, n} \gamma_I^{m, n} e^{\alpha_{mn} I \tau} \left( \frac{s}{s_0} \right)^{\alpha_m(\tau) + \alpha_n(\tau)}, \quad (6.2)$$

or, with linear trajectories, to an integrated elastic cross section

$$\begin{aligned} \sum_{I'} \beta_{II'} \sigma_{I, \text{el}} \\ \propto \frac{1}{s^2} \sum_{m, n} \gamma_I^{m, n} \frac{(s/s_0)^{\alpha_m(0) + \alpha_n(0)}}{a_{mn}^I + (\alpha_m' + \alpha_n') \ln(s/s_0)}. \end{aligned} \quad (6.3)$$

The form (6.3) evidently leads to (6.1) through the identifications

$$\beta_i = \alpha_m(0) + \alpha_n(0) - 1 \quad (6.4)$$

and

$$b_i^I = \frac{a_{mn}^I}{\alpha_m' + \alpha_n'}. \quad (6.5)$$

Since the isospin in question refers to the crossed reaction, the leading trajectory combinations for  $I=0$  are  $PP$ ,  $PP'$ ,  $\rho\rho$ , and  $P'P'$ . For  $I=1$ , the leading combinations are  $P\rho$ ,  $P'\rho$ , and  $\rho\rho$ , and for  $I=2$  we have  $\rho\rho$ .

For  $D^I(\lambda)$ , in the trace approximation, we now write

$$D^I(\lambda) \approx 1 - T_{\text{res}}^I(\lambda) - T_{\text{asym}}^I(\lambda), \quad (6.6)$$

where

$$\begin{aligned} T_{\text{res}}^I(\lambda) &= \frac{1}{\lambda + 1} \int_{-\Delta}^0 \frac{dt}{(t - m_\pi^2)^2} \int_{4m_\pi^2}^{s^*} ds \\ &\quad \times e^{-(\lambda+1)\eta(s,t)} C^I(s), \end{aligned} \quad (6.7)$$

$$T_{\text{asym}}^I(\lambda) = \frac{1}{\lambda+1} \sum_i C_i^I \int_{-\Delta}^0 \frac{dt}{(t-m_\pi^2)^2} \int_{s^*}^{\infty} ds \times \frac{e^{(-\lambda+1)\eta(s,t)}}{b_i^I + \ln(s/s_0)} \left(\frac{s}{s_0}\right)^{\beta_i}. \quad (6.8)$$

To evaluate  $T_{\text{asym}}^I(\lambda)$  we note that, since  $s$  is much larger than  $t$ ,  $e^\eta \approx (-s/t)$ . This gives

$$T_{\text{asym}}^I(\lambda) \approx \frac{1}{\lambda+1} \int_{-\Delta}^0 dt \frac{(-t)^{\lambda+1}}{(t-m_\pi^2)^2} \sum_i C_i^I \int_{s^*}^{\infty} ds \times \frac{s^{-(\lambda+1)}(s/s_0)^{\beta_i}}{b_i^I + \ln(s/s_0)}. \quad (6.9)$$

If  $\lambda$  is not too close to zero, we may neglect the  $m_\pi^2$  in the  $t$  integration. Then performing the  $t$  integration and changing variables in the  $s$  integral, we have

$$T_{\text{asym}}^I(\lambda) = \frac{(\Delta/s_0)^\lambda}{\lambda(\lambda+1)} \sum_i C_i^I e^{b_i^I(\lambda-\beta_i)} \times \int_{(\lambda-\beta_i)[b_i^I + \ln(s^*/s_0)]}^{\infty} dx \frac{e^{-x}}{x} = \frac{(\Delta/s_0)^\lambda}{\lambda(\lambda+1)} \sum_i C_i^I e^{b_i^I(\lambda-\beta_i)} \times E_1 \left[ (\lambda-\beta_i) \left( b_i^I + \ln \frac{s^*}{s_0} \right) \right]. \quad (6.10)$$

In the integral form one can see the expected logarithmic singularity.

Turning to the resonance component (6.7), it is difficult to avoid a numerical  $s$  integration, but because the range of  $s$  is restricted, we no longer need a cutoff in  $t$ . Inverting the order of integration and again setting  $m_\pi^2=0$ , we have

$$T_{\text{res}}^I(\lambda) \approx \frac{1}{\lambda+1} \int_{4m_\pi^2}^{s^*} ds C^I(s) \int_{-\infty}^0 \frac{dt}{t^2} e^{-(\lambda+1)\eta(s,t)} = \frac{2}{\lambda(\lambda+1)(\lambda+2)} \int_{4m_\pi^2}^{s^*} \frac{ds}{s} C^I(s). \quad (6.7')$$

It appears that the leading  $\lambda$  singularity here is at  $\lambda=0$ , a surprising result, since the more correct expression (6.7) has only the pole at  $\lambda=-1$  that arose from pion exchange ( $2\alpha_\pi-1=-1$ ). The pole in (6.7') at  $\lambda=0$  arises from the approximation of setting  $m_\pi^2=0$ , a simplification unjustified for  $\lambda \lesssim 0$ . As before, however, we shall be chiefly interested in the region where  $\lambda \gtrsim \frac{1}{2}$ .

Combining the preceding results, we have

$$D^I(\lambda) \approx 1 - \frac{1}{\lambda(\lambda+1)} \left\{ \frac{2}{\lambda+2} R_I + \left(\frac{\Delta}{s_0}\right)^\lambda \sum_i C_i^I e^{b_i^I(\lambda-\beta_i)} \times E_1 \left[ (\lambda-\beta_i) \left( b_i^I + \ln \frac{s^*}{s_0} \right) \right] \right\}, \quad (6.11)$$

where

$$R_I = \int_{4m_\pi^2}^{s^*} \frac{ds}{s} C^I(s). \quad (6.12)$$

Formula (6.11) above may be compared with the denominator appearing in Eq. (4.2) of Ref. 5 to relate the ABFST model to that of CP. To show more clearly the relation between the models, we keep only the leading cut and then make a pole approximation for this cut. That is, we assume  $b_i^I$  to be large and use the asymptotic expansion of the exponential integral,

$$E_1(z) \sim \frac{e^{-z}}{z} \left[ 1 - \frac{1}{z} + O\left(\frac{1}{z^2}\right) \right] \sim \frac{e^{-z}}{z+1}, \quad (6.13)$$

to get

$$D^I(\lambda) = 1 - \frac{1}{\lambda(\lambda+1)} \left\{ \frac{2}{\lambda+2} R_I + \left(\frac{\Delta}{s_0}\right)^\lambda \left[ \frac{C^I}{b^I + \ln(s^*/s_0)} \times \frac{\exp[-(\lambda-\beta_I) \ln(s^*/s_0)]}{\lambda-\beta_I+1/[b^I + \ln(s^*/s_0)]} \right] \right\} \quad (6.14)$$

for

$$\lambda - \beta_I \gg \frac{1}{b^I + \ln(s^*/s_0)}.$$

Thus the cut with a branch point at  $\beta_I$  and discontinuity proportional to  $e^{b(\lambda-\beta)}$  is replaced by a pole at

$$\bar{\beta}_I = \beta_I - \frac{1}{b^I + \ln(s^*/s_0)}, \quad (6.15)$$

the approximate "center of gravity" of the discontinuity.

Restricting discussion to  $I=0$ , where we are approximating the  $PP$  cut by a pole, we have, from (2.3a'),

$$C_0(s) \underset{s>s^*}{\approx} (s/16\pi^3) \left[ \frac{1}{3} \sigma_{I_{s=0}^{\text{el}}}(s) + \sigma_{I_{s=1}^{\text{el}}}(s) + (5/3) \sigma_{I_{s=2}^{\text{el}}}(s) \right] \approx (3s/16\pi^3) \sigma^{\text{el}}(s), \quad (6.16)$$

and thus the single-term approximation

$$C_0(s) \approx \frac{C^0}{b^0 + \ln(s/s_0)} \left(\frac{s}{s_0}\right)^{\beta_0} \quad (6.17)$$

corresponds, with  $\beta_0 \approx 1$ , to

$$\frac{3s_0}{16\pi^3} \sigma^{\text{el}}(s) \approx \frac{C^0}{b^0 + \ln(s/s_0)}. \quad (6.18)$$

Thus the coefficient within the square bracket in (6.14) may be evaluated as

$$\frac{C^0}{b^0 + \ln(s^*/s_0)} \approx \frac{3s_0}{16\pi^3} \sigma^{e1}(s^*), \quad (6.19)$$

allowing (6.14) for  $I=0$  to be written as

$$D^0(\lambda) \approx 1 - \frac{1}{\lambda(\lambda+1)} \left[ \frac{2}{\lambda+2} R_0 + \left( \frac{\Delta}{s_0} \right)^\lambda \left( \frac{3s_0 \sigma^{e1}(s^*)}{16\pi^3} \right) \times \frac{\exp[-(\lambda-\beta_0) \ln(s^*/s_0)]}{\lambda - \bar{\beta}_0} \right]. \quad (6.20)$$

For comparison with the CP model, we now consider the denominator of Eq. (4.2) of Ref. 5 (identifying  $J$  with  $\lambda$ ),

$$D(\lambda) = 1 - g_M^2 \rho^M(\lambda) - g_{P^4} \rho^P(\lambda) \rho^M(\lambda), \quad (6.21)$$

where the propagator functions  $\rho^i(\lambda)$  are normalized to  $(\lambda - \beta_i)^{-1}$  for  $\lambda - \beta_i$  large. The corresponding functions of  $\lambda$  in (6.20) fall off more rapidly than the inverse first power, but the resonance component of (6.20) decreases smoothly after the pole at  $\lambda=0$ , and the high-energy component decreases smoothly after the pole at  $\lambda = \bar{\beta}_0$ . We are chiefly interested in the region near  $\lambda=1$ , so let us replace all but these leading-pole factors in (6.20) by the values taken at  $\lambda=1$ . Then (6.20) becomes

$$D^0(\lambda) \underset{\lambda \text{ near } 1}{\approx} 1 - \frac{1}{\lambda} \left[ \frac{1}{3} R_0 + \frac{1}{2} \left( \frac{\Delta}{s_0} \right) \left( \frac{3s_0 \sigma^{e1}(s^*)}{16\pi^3} \right) \times \frac{1}{\lambda - \bar{\beta}_0} \right]. \quad (6.22)$$

Comparing (6.21) with (6.22), we may now read off the following rough equivalences:

$$\beta_M \approx 0, \quad (6.23)$$

$$\beta_P \approx \bar{\beta}_0, \quad (6.24)$$

$$g_M^2 \approx \frac{1}{3} R_0, \quad (6.25)$$

$$g_{P^4} \approx \frac{1}{2} \left( \frac{\Delta}{s_0} \right) \frac{3s_0 \sigma^{e1}(s^*)}{16\pi^3}. \quad (6.26)$$

It is interesting to remark that  $\beta_M \approx 0$  means, according to Eq. (6.4), that in the CP model an input-pion trajectory behaves like  $\alpha_\pi(0) \approx \frac{1}{2}$  rather than  $\alpha_\pi(0) = 0$ . An equivalent statement is that an inelastic two-body-to-two-body cross section with pion exchange varies as  $s^{-1}$ , not  $s^{-2}$ , for  $s$  not too large. Such a cross section is given by

$$\sigma^{AB \rightarrow CD}(s) \propto s^{-2} \int_{-\infty}^{t_{\min}} dt \frac{1}{(t - m_\pi^2)^2} \propto \frac{s^{-2}}{m_\pi^2 - t_{\min}}.$$

Since

$$t_{\min} \approx -(m_C^2 - m_A^2)(m_D^2 - m_B^2)/s,$$

it follows that when  $s$  is small enough that  $|t_{\min}| \gg m_\pi^2$ ,

$$\sigma^{AB \rightarrow CD}(s) \propto s^{-1}.$$

The result (6.26) provides an estimate of the internal Pomeron coupling in terms of the elastic  $\pi\pi$  cross section. Previously we estimated  $\sigma_{e1\pi\pi} = 2.5 - 3.0$  mb for  $= 20 - 50$  GeV<sup>2</sup>. Since  $s^* = 3$  GeV<sup>2</sup>, it may be that  $\sigma_{e1\pi\pi}(s^*)$  (actually just the Pomeron contribution to it) is slightly larger, perhaps 3.5 mb. This estimate gives, for  $g_{P^4}$ ,

$$g_{P^4} \approx 0.03 \Delta \text{ GeV}^{-2}. \quad (6.27)$$

Therefore our assumptions,  $\Delta \lesssim 1$  GeV<sup>2</sup>, implies a small value for  $g_{P^4}$ , small enough to justify making a crude model by dropping the Pomeron component of the kernel. It should be obvious to the reader that we are here repeating the estimate of Sec. IV, but now in a “ $J$ -plane language.”

The estimate (6.27) is in satisfactory accord with the requirements of Ref. 20, where the small high-energy tail of the kernel is used in a CP-type model to split the leading output pole into  $P$  plus  $P'$ . Such a splitting capability requires  $g_{P^4} \approx 0.03$ .

In papers employing the CP model,<sup>1,4,5</sup> it has been shown that the large experimentally observed multiplicity implies that the effective output pole should be produced primarily by the low-energy component of the kernel. Neglecting  $g_{P^4}$ , or dropping the contribution to the trace from  $s > s^*$  in the more accurate equation (6.11), leads to

$$D^I(\lambda) \approx 1 - 2R_I/\lambda(\lambda+1)(\lambda+2). \quad (6.28)$$

To produce the  $P$  and  $\rho$  poles we evidently need to have

$$D^0(\lambda \approx 1) = 0 \quad \text{and} \quad D^1(\lambda \approx \frac{1}{2}) = 0. \quad (6.29)$$

By numerically integrating  $C^I(s)/s$  (see Fig. 4), one obtains, from Eq. (6.12),  $R_0 = 0.79$ ,  $R_1 = 0.31$ , and  $R_2 = 0.01$  for  $s^* = 3$  GeV<sup>2</sup>. The first two values are too small by a factor of 3 to 4 to satisfy (6.29). Correspondingly, evaluation of  $g_M^2$  from Eq. (6.25) leads to  $g_M^2 \approx \frac{1}{4}$ , whereas in CP,<sup>1</sup>  $g_M^2$  needs to be  $\approx 1$ .

In Ref. 20 we show for  $I=0$  that it is unnecessary for the low-energy component of the kernel to produce a pole as high as  $\lambda=1$ . If the kernel with only the low-energy contribution can, via Eq. (6.28), produce a pole at  $\lambda=0.7$ , then addition of the high-energy-kernel tail can boost the leading singularity to  $\lambda \approx 1$  and still maintain an acceptable multiplicity. Assuming such to be the requirement,  $R_0 \approx 0.8$  is seen to be roughly half of what is needed.

<sup>20</sup> G. F. Chew and D. R. Snider, Phys. Rev. D **1**, 3453 (1970).

Although the  $R_I$ 's calculated from Eq. (6.12) are too small, they have the proper ratio to explain the observed ordering of the leading  $I=0, 1,$  and  $2$  trajectories. In Appendix C we point out that such is not the case for a purely multi-Regge model based on duality.

## VII. SUMMARY AND DISCUSSION

We began this paper by arguing that the ABFST model has a firmer physical basis than multi-Regge models, and we have explored various aspects of the ABFST model to illuminate in particular the CP multi-Regge model. We have confirmed the notion of a weak Pomeron component in the multiperipheral kernel, relating this idea to the small d.d. cross section and obtaining an estimate for the CP Pomeron coupling constant in terms of the high-energy elastic  $\pi\pi$  cross section. The lower-trajectory aspects of the multi-Regge kernel have been found to have weaker physical foundation, duality giving a poor representation of the important resonance components of the ABFST kernel. Nevertheless, if one foregoes direct identification of input and output poles, it is possible to find input poles for the CP model which roughly simulate the important resonance input of the ABFST model. The factorizability of the CP kernel, although motivated originally by an illegitimate assumption of large subenergies, appears not to be grossly misleading.

In the course of the investigation, unanticipated light was shed on several matters. (a) We discovered a generalization of the Berestetsky-Pomeranchuk formula which provides a practical basis for exact numerical evaluation of the ABFST model at any energy. (b) We found a way of looking at diffractive dissociation which explains certain paradoxical features of this concept. (c) We found that the exceptionally small pion mass causes the pion-exchange effect in a CP-type multi-Regge model to act like a trajectory with  $J \approx \frac{1}{2}$  rather than  $J=0$ .

A disappointing discovery was the deficient strength, by a factor 2 to 3, of the resonance component of the ABFST kernel, based on a reasonable estimate of the  $\pi\pi$  cross section. We can offer several possible explanations for this deficiency, the most immediate being the inherent limitation of the model. The basis of the model is the presence in the multiparticle production amplitude of pion poles, with residues that are related to the elastic  $\pi\pi$  amplitude. This fact suggests, but does not determine, the multiparticle amplitude in its physical region.<sup>21</sup>

A second possible factor contributing to the inadequate kernel strength is our estimate of the  $\pi\pi$  elastic cross section. For example, Wolf,<sup>22</sup> in fitting reactions with pion exchange, used  $\pi\pi$  cross sections which were 6 to 8 times as large as ours at threshold. Another possible source of error is interference terms (crossed graphs).<sup>23</sup> Since the mean  $\pi\pi$  subenergies are comparable to the momentum transfers, the usual motivation for neglecting crossed diagrams is diminished.

In spite of the inadequate kernel strength, the qualitative characteristics of the ABFST model seem impressively relevant to nature. With a "fudge factor" to augment the resonance component, we expect that this original version of the multiperipheral model will prove extremely useful.

## ACKNOWLEDGMENTS

Extensive discussions with James S. Ball, G. Marchesini, and Don Tow have been of major assistance in the work reported here.

## APPENDIX A: GENERALIZATION OF BERESTETSKY-POMERANCHUK FORMULA

The general cross-section formula for producing  $n$  particles is [see Fig. 7(a)]

$$\sigma_{2 \rightarrow n}(s) = \frac{(2\pi)^4}{2\lambda(s, m_A^2, m_B^2)} \prod_{i=1}^n \int \frac{d^4 k_i \delta^+(k_i^2 - m_i^2)}{(2\pi)^3} \delta^4(p_A + p_B - \sum_{i=1}^n k_i) |A_{2 \rightarrow n}|^2. \quad (\text{A1})$$

For the ABFST model, we group the final particles into  $N+2$  pairs and use a different labeling system, as shown

<sup>21</sup> Various alternative "off-shell continuations" for the ABFST resonance kernel have been considered by D. Tow, Phys. Rev. D **2**, 154 (1970). The strip model is a different version of a multiperipheral model, based on  $\pi\pi$  amplitudes, which does not exhibit an "off-shell ambiguity." According to recent calculations by P. D. B. Collins and R. Johnson [Phys. Rev. **185**, 2020 (1969); **177**, 2472 (1969)], the resonance input to the strip model has adequate strength.

<sup>22</sup> Gunter Wolf, Phys. Rev. **182**, 1538 (1969).

<sup>23</sup> Any finite number of crossed diagrams could be generated by a more general kernel which still maintains the basic structure of the integral equation.

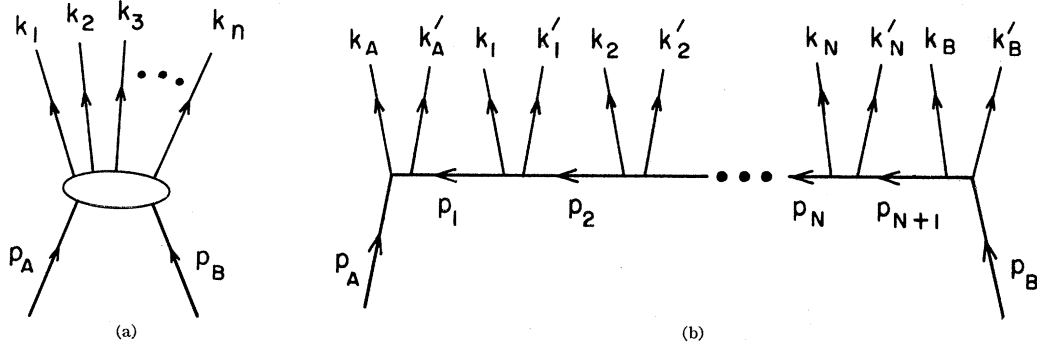


FIG. 7. (a) Diagram showing significance of momentum labels in Eq. (A1); (b) diagram showing significance of momentum labels in Eq. (A2).

in Fig. 7(b). With the factored reaction amplitude (1.2), the corresponding cross-section formula is

$$\begin{aligned} \sigma_{N^{AB}}(s) = & \frac{(2\pi)^4}{2\lambda(s, m_A^2, m_B^2)} \int \frac{d^4 k_A \delta^+(k_A^2 - m_A^2)}{(2\pi)^3} \int \frac{d^4 k'_A \delta^+(k_A'^2 - m_\pi^2)}{(2\pi)^3} |f_A(s_A, \theta_A)|^2 \prod_{i=1}^N \int \frac{d^4 k_i \delta^+(k_i^2 - m_\pi^2)}{(2\pi)^3} \\ & \times \int \frac{d^4 k'_i \delta^+(k_i'^2 - m_\pi^2)}{(2\pi)^3} |f(s_i, \theta_i)|^2 \int \frac{d^4 k_B \delta^+(k_B^2 - m_\pi^2)}{(2\pi)^3} \int \frac{d^4 k'_B \delta^+(k_B'^2 - m_\pi^2)}{(2\pi)^3} |f_B(s_B, \theta_B)|^2 \\ & \times \delta^4(p_A + p_B - K_A - K_B - \sum_{i=1}^N K_i) \prod_{i=1}^{N+1} \frac{1}{(t_i - m_\pi^2)^2}, \quad (\text{A2}) \end{aligned}$$

where

$$s_j = K_j^2 \quad \text{with} \quad K_j = k_j + k'_j, \quad t_j = p_j^2,$$

with  $p_j$  defined as in Fig. 7(b), and  $\theta_j$  is the angle between  $k_j$  and  $p_j$  in the  $K_j$  rest frame. Note the important fact that the momentum transfers  $p_j$  can be expressed entirely in terms of the  $K_j$ .

Consider in Eq. (A2) the factors associated with a particular pair of outgoing particles, adding a formal integration over  $d^4 K_j$ , together with a compensating  $\delta$  function:

$$\int d^4 K_j \int \frac{d^4 k_j \delta^+(k_j^2 - m_\pi^2)}{(2\pi)^3} \int \frac{d^4 k'_j \delta^+(k_j'^2 - m_\pi^2)}{(2\pi)^3} |f(s_j, \theta_j)|^2 \delta^4(k'_j + k_j - K_j). \quad (\text{A3})$$

For a fixed  $K_j$ , the integration here over  $d^4 k_j d^4 k'_j$  is evidently identical to that which occurs in the corresponding elastic cross section. Expression (A3) consequently can be written

$$\int d^4 K_j \frac{2\lambda(s_j, m_\pi^2, m_\pi^2)}{(2\pi)^4} \sigma_{\text{el}}^{\pi\pi}(s_j),$$

which with the definition (2.3a) becomes

$$\frac{2}{\pi} \int d^4 K_j C(s_j) = \frac{2}{\pi} \int ds_j C(s_j) \int d^4 K_j \delta^+(K_j^2 - s_j), \quad (\text{A3}')$$

a corresponding rule also holding for the  $A$  and  $B$  pairs at the ends of the chain. Equation (A2) may thus be contracted to

$$\begin{aligned} \sigma_{N^{AB}}(s) = & \frac{(2\pi)^4}{2\lambda(s, m_A^2, m_B^2)} \left(\frac{2}{\pi}\right)^{N+2} \int ds_A C_A(s_A) \int ds_1 C(s_1) \cdots \int ds_B C_B(s_B) \int d^4 K_A \delta^+(K_A^2 - s_A) \\ & \times \int d^4 K_1 \delta^+(K_1^2 - s_1) \cdots \int d^4 K_B \delta^+(K_B^2 - s_B) \delta^4(p_A + p_B - K_A - K_B - \sum_{i=1}^N K_i) \prod_{i=1}^{N+1} \frac{1}{(t_i - m_\pi^2)^2}. \quad (\text{A2}') \end{aligned}$$

The region of integration for the  $K_j$  in (A2') is just the usual phase space for  $N+2$  "particles" with "masses"  $(s_j)^{1/2}$ . The region of integration for the  $s_j$  is more subtle. The lower limit for each  $s_j$  is simply the appropriate elastic threshold, but the upper limit is collectively determined by the requirement that

$$(s_A)^{1/2} + (s_B)^{1/2} + \sum_{i=1}^N (s_i)^{1/2} \leq (s)^{1/2}. \quad (\text{A4})$$

With a change of variables from the  $K_j$  to the  $p_j$ , thereby eliminating the energy-momentum conservation  $\delta$  function, Eq. (A2') constitutes the basis for Sec. III.

To derive Eq. (2.5) from (A2'), we note that for a fixed set of  $s_j$  the integration over the  $K_j$ 's amounts to just the  $(N+2)$ -particle phase space. We treat this problem as a succession of two-particle phase-space calculations, starting at the  $B$  end of the chain. Thus we first consider  $K_B$  as one "particle," the other "particle" consisting of all remaining pairs, with combined momentum (see Fig. 8)

$$\tilde{K}_{N+1} = K_A + K_1 + \cdots + K_N.$$

This two-particle phase space may be calculated as

$$\int d^4 K_B \delta^+(K_B^2 - s_B) d^4 \tilde{K}_{N+1} \delta^+(\tilde{K}_{N+1}^2 - v_{N+1}) \delta^4(p_A + p_B - K_B - \tilde{K}_{N+1}) = \frac{1}{2\pi} \frac{1}{\lambda(s, m_A^2, m_B^2)} \int dt_{N+1}, \quad (\text{A5})$$

the angular integrations having been performed in the absence of any factors in the model that depend on angles. In (A5) we have introduced a factor  $\delta^+(\tilde{K}_{N+1}^2 - v_{N+1})$  which does not appear in (A2') and so, to compensate, we must integrate over  $dv_{N+1}$ . We also have introduced  $d^4 \tilde{K}_{N+1}$ , which we compensate with a factor  $\delta^4(\tilde{K}_{N+1} - K_A - K_1 - \cdots - K_N)$  that carries over to the next step, where we consider  $K_N$  as one "particle" and  $\tilde{K}_N = K_A + K_1 + \cdots + K_{N-1}$  as the other "particle." The next two-particle phase-space calculation then leads to

$$\frac{1}{2\pi} \frac{1}{\lambda(v_{N+1}, m_A^2, t_{N+1})} \int dt_N, \quad (\text{A6})$$

together with an integration over  $dv_n$ . Repeating the process down to the  $A$  end of the chain, we have

$$\begin{aligned} & \int d^4 K_A \delta^+(K_A^2 - s_A) \int d^4 K_1 \delta^+(K_1^2 - s_1) \cdots \int d^4 K_B \delta^+(K_B^2 - s_B) \delta^4(p_A + p_B - K_A - K_1 - \cdots - K_B) \\ &= \frac{\pi}{2\lambda(s, m_A^2, m_B^2)} \int dv_{N+1} dt_{N+1} \frac{\pi}{2\lambda(v_{N+1}, m_A^2, t_{N+1})} \int dv_N dt_N \cdots \\ & \quad \frac{\pi}{2\lambda(v_3, m_A^2, t_3)} \int dv_2 dt_2 \frac{\pi}{2\lambda(v_2, m_A^2, t_2)} \int dt_1. \quad (\text{A7}) \end{aligned}$$

The final step is to integrate over the  $v$ 's. Here the use of Toller variables is appropriate. In addition to the boosts defined by Eqs. (2.1a) and (2.2), we define the parameter  $\zeta_i$ ,

$$\sinh \zeta_i = \frac{v_i - m_A^2 - t_i}{2m_A(-t_i)^{1/2}}, \quad \cosh \zeta_i = \frac{\lambda(v, m_A^2, t_i)}{2m_A(-t_i)^{1/2}}, \quad (\text{A8})$$

which boosts from the rest frame of particle  $A$  where  $p_i$  is "z-t like" to the frame where  $p_i$  is "z like" and  $p_A$  is "z-t like." (By our numbering convention  $\zeta_1 = q_A$ .) We also require the parameter  $\xi_i$ , which boosts from the latter frame to the frame where  $p_i$  is still "z like" but  $p_{i+1}$  is "z-t like." The relation among these Toller

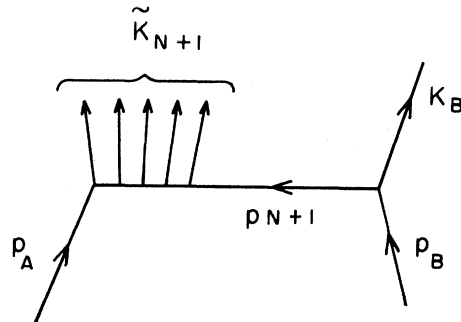


FIG. 8. Momentum diagram defining the "cluster momenta"  $\tilde{K}_i$  used to express multiparticle phase space as a product of two-body phase spaces.

variables is

$$\sinh\zeta_{i+1} = \sinh\zeta_i \cosh q_i \cosh \xi_i + \cosh\zeta_i \sinh q_i, \quad (\text{A9})$$

$$\cosh\eta = \sinh\zeta_{N+1} \sinh q_B \cosh \xi_{N+1} + \cosh\zeta_{N+1} \cosh q_B. \quad (\text{A10})$$

Since each  $\xi_i$  has a zero lower limit,  $\zeta_{i+1}$  has a lower limit equal to  $\zeta_i + q_i$ , while in addition  $\zeta_{N+1}$  has an upper limit equal to  $\eta - q_B$ .

Observe now from (A8) that, for fixed  $t_i$ ,

$$\frac{dv_i}{\lambda(v_i, m_A^2, t_i)} = \frac{d \sinh\zeta_i}{\cosh\zeta_i} = d\zeta_i. \quad (\text{A11})$$

It then follows that

$$\begin{aligned} & \int \frac{dv_{N+1}}{\lambda(v_{N+1}, m_A^2, t_{N+1})} \cdots \int \frac{dv_2}{\lambda(v_2, m_A^2, t_2)} \\ &= \int_{q_A + q_1 + \cdots + q_N}^{\eta - q_B} d\zeta_{N+1} \cdots \int_{q_A + q_1 + q_2}^{\zeta_4 - q_3} d\zeta_3 \int_{q_A + q_1}^{\zeta_3 - q_2} d\zeta_2 \\ &= (1/N!) (\eta - q_A - q_1 - \cdots - q_N - q_B)^N \\ & \quad \times \theta(\eta - q_A - q_1 - \cdots - q_N - q_B). \quad (\text{A12}) \end{aligned}$$

Insertion of (A12) into (A7) and thence into (A2') leads to the form (2.5) presented in the text.

### APPENDIX B: ASYMPTOTIC PHASE-SPACE SIMPLIFICATION FOR DIFFRACTIVE DISSOCIATION FORMULA (4.8)

The large- $s$  limit of the integrals appearing in Eq. (4.8) can be evaluated in closed form if one realizes that, because of the small pion mass the exterior vertex boosts are always large, while the interior vertex (when it occurs) involves only  $s_i > s^*$  and also, therefore, only large boosts. We may consequently replace  $2 \sinh q_i$  or  $2 \cosh q_i$  by  $e^{q_i}$ , as well as  $2 \cosh \eta$  by  $e^\eta$ . We may furthermore simplify (2.2) to

$$\cosh q_2 \approx s_2 / 2(t_1 t_2)^{1/2}$$

at an interior vertex, while (2.1b) leads to

$$\sinh q_1 \approx (s_1 - t_1) / 2m_\pi (-t_1)^{1/2},$$

with a corresponding simplification at the other exterior vertex. There is, of course, never any question about the approximation

$$2 \cosh \eta \approx s / m_\pi^2.$$

Thus in the first term of (4.8) we employ the simplification

$$\eta - q_1 - q_2 \approx \ln \frac{s(-t)}{(s_1 - t)s_2},$$

where even the  $t$  in the denominator will be dropped for

$s_1 > s^*$ , while in the second term of (4.8) we use

$$\eta - q_1 - q_2 - q_3 \approx \ln \frac{st_1 t_2}{(s_1 - t_1)s_2(s_3 - t_2)},$$

again dropping a denominator  $t$  whenever the companion  $s_i$  is large.

Making the one additional and unquestionably legitimate approximation of setting the pion mass equal to zero in the propagators, it is then possible to evaluate the integrals in closed form.

### APPENDIX C: DUALITY AND KERNEL OF ABFST INTEGRAL EQUATION

When the first multi-Regge model was proposed, it was suggested that through "duality" the Regge form might represent the resonance region in some average sense. At that time, however, it was not appreciated how low the average subenergy actually is. Given that the average subenergy is  $s \lesssim 1 \text{ GeV}^2$ ,<sup>9</sup> the applicability of duality to the multiperipheral model becomes more doubtful. We shall show here that one realization of the duality concept, based on the Veneziano model, leads to a qualitatively wrong isospin dependence of the ABFST kernel.

The Veneziano model for  $\pi\pi$  scattering<sup>24,25</sup> contains both  $\rho$  and  $P'$  trajectories. Because of the absence of  $I=2$  resonances, these trajectories are exchange degenerate, a fact which fixes the ratio of their residues and consequently fixes the ratio of the three ABFST kernels. The Veneziano model gives for the  $s$ -channel  $\pi\pi$  amplitudes

$$A_{I_s=0} = \frac{1}{2} [3B(s,t) + 3B(s,u) - B(t,u)],$$

$$A_{I_s=1} = B(s,t) - B(s,u),$$

and

$$A_{I_s=2} = B(t,u),$$

where

$$B(s,t) = \frac{\beta \Gamma(1-\alpha(s)) \Gamma(1-\alpha(t))}{\Gamma(1-\alpha(s)-\alpha(t))}.$$

Except for the unfortunate  $\rho'$ , this model contains the same resonances with roughly the same properties as we use in Table I for the low-energy  $\pi\pi$  cross sections.

To test the usefulness of duality in the multiperipheral model, we take the asymptotic form of the Veneziano model, and then use it, even in the low-energy region, to determine the kernel. The large- $s$  asymptotic form is

$$A_{I_s=0} \sim \beta \Gamma(1-\alpha(t)) (s/s_0)^{\alpha(t)} \left( \frac{3}{2} e^{-i\pi\alpha(t)} - \frac{1}{2} \right),$$

$$A_{I_s=1} \sim \beta \Gamma(1-\alpha(t)) (s/s_0)^{\alpha(t)} e^{-i\pi\alpha(t)},$$

<sup>24</sup> C. Lovelace, Phys. Letters **28B**, 264 (1968).

<sup>25</sup> J. Shapiro, Phys. Rev. **179**, 1345 (1969).

and

$$A_{I_s=2} \sim \beta \Gamma(1-\alpha(l)) (s/s_0)^{\alpha(l)}.$$

Notice that the Regge form of  $A_{I_s=2}$  is real, a result which, by duality, is necessary if the  $I_s=2$  channel is to have no resonances. On the other hand, when we square the amplitudes to get the isospin cross sections, we will obviously get equal  $I_s=1$  and  $I_s=2$  cross sections. Comparing with our estimated cross sections, Fig. 4(a), we see that we must expect difficulties.

Neglecting this forewarning and continuing, we find, for the differential cross sections needed in (6.2),

$$\frac{d\sigma_{I_s=0}^{e1}}{d\tau} = \frac{1}{2}\pi\beta^2\Gamma^2(1-\alpha(\tau))\left(\frac{s}{s_0}\right)^{2\alpha(\tau)-2} \times \{3 \sin^2[\frac{1}{2}\pi\alpha(\tau)] + 1\},$$

$$\frac{d\sigma_{I_s=1}^{e1}}{d\tau} = \frac{d\sigma_{I_s=2}^{e1}}{d\tau} = \frac{1}{2}\pi\beta^2\Gamma^2(1-\alpha(\tau))\left(\frac{s}{s_0}\right)^{2\alpha(\tau)-2}.$$

To obtain the  $C^I$ 's, Eq. (2.3a'), we cross to the  $l$  channel before doing the  $\tau$  integration and find

$$\begin{pmatrix} C^0 \\ C^1 \\ C^2 \end{pmatrix} = \frac{\lambda(s, m_\pi^2, m_\pi^2)}{16\pi^3} \int d\tau \Gamma^2(1-\alpha(\tau)) \left(\frac{s}{s_0}\right)^{2\alpha(\tau)-2} \times \begin{pmatrix} 3 + \sin^2[\frac{1}{2}\pi\alpha(\tau)] \\ \sin^2[\frac{1}{2}\pi\alpha(\tau)] \\ \sin^2[\frac{1}{2}\pi\alpha(\tau)] \end{pmatrix}.$$

Since  $\alpha(0) \approx \frac{1}{2}$ , the values of the integrands at  $\tau=0$  (at the forward peak) are in the ratio 7:1:1 for  $I=0, 1$ , and 2, respectively. Taking the different widths of the forward peaks into account, we see that  $C^0, C^1$ , and  $C^2$  are in the ratio  $r:1:1$  with  $r > 7$ . This implies that the low-energy contributions to the kernel—the parts with no singularity for  $\lambda > 0$ —also stand in the ratio  $r:1:1$ . These ratios can be compared with those calculated directly from the low-energy resonances, where we found the  $R_I$  to stand in the ratio 0.79:0.31:0.01.

We see that the naive use of duality leads to the disastrous prediction that output  $I=1$  and  $I=2$  poles occur at the same value of  $\lambda$ . It also will probably lead to an excessively large separation between the output  $I=0$  and  $I=1$  poles.

## Induction of Quarklike Structure of Baryons\*

RICHARD H. CAPPS

*Physics Department, Purdue University, Lafayette, Indiana 47907*

(Received 10 April 1970)

A set of self-consistency conditions for the interactions of a hypothetical set of even- and odd-parity mesons and baryons is studied. These conditions, previously derived, are written in a form that makes some of their implications transparent. Two types of  $SU(n)$ -invariant solutions are found; in only one of these do baryon exchanges participate in the bootstrapping of the baryons. The conditions imply that the meson-baryon-baryon interactions are proportional to matrix elements of the group generators in the space of a single quark, yet the identification of baryons with simple quarks does not lead to a solution. Thus, the baryons may be regarded as composites containing quarks. An approximate solution based on the  $SU(6)$  group may correspond to experiment better than any exact solution.

### I. INTRODUCTION

TWO years ago, the author used fixed-angle dispersion relations and a simple dynamical assumption to derive bootstrap consistency conditions on the ratios of the trilinear coupling constants of a hypothetical set of mesons and baryons of both parities.<sup>1,2</sup> Recently, a slight modification of this set of consistency conditions was obtained from an idealized Veneziano model.<sup>3</sup> In this latter derivation, the "particles" are

\* Supported in part by the U. S. Atomic Energy Commission.

<sup>1</sup> R. H. Capps, Phys. Rev. **168**, 1731 (1968). This paper is referred to as R1.

<sup>2</sup> R. H. Capps, Phys. Rev. **171**, 1591 (1968). This paper is referred to as R2.

<sup>3</sup> R. H. Capps, Phys. Rev. D **1**, 2395 (1970). This paper is referred to as R3.

the lightest particles on Regge trajectories. In Ref. 3 (R3), an  $SU(3)$ -symmetric solution to these conditions was found, involving singlets, octets, and a decuplet.

In the present paper, the bootstrap conditions of R3 are written in a more elegant form. This enables us to generalize the solution of R3 to the symmetry group  $SU(n)$ . The new form makes it clear (as shown in Sec. III) that any solution must have many of the features of the quark model. It may be that dynamical consistency conditions are the reason that the quark model works.

The most physical solution corresponds to the group  $SU(6)$ , and is discussed in Sec. IV. The baryon trajectories correspond to the  $SU(6)$  multiplets and parities  $56^+$ ,  $70^+$ ,  $70^-$ , and  $20^-$ . An approximate solu-